Reorganization of Resting-State Functional Connectivity with a Feature-Representation Region after Visual Perceptual Training

by

Taghizadeh Sarabi Mitra

Student ID Number: 1196008

A dissertation submitted to the
Engineering Course, Department of Engineering,
Graduate School of Engineering,
Kochi University of Technology,
Kochi, Japan

in partial fulfillment of the requirements for the degree of
Doctor of Philosophy

Assessment Committee:
      Supervisor: Kiyoshi Nakahara
      Co-Supervisor: Xiangshi Ren, Kochi University of Technology
      Co-Supervisor: Shinichi Yoshida, Kochi University of Technology
      Kiminori Matsuzaki
      Nobuhiro Mifune

March 2018

ABSTRACT

Reorganization of Resting-State Functional Connectivity with a Feature-Representation Region after Visual Perceptual Training: an fMRI Study

How quickly and accurately we extract important signals from our highly complex environment and making decisions rely on our perceptual ability [3]. Training or repeated exposure to a specific feature can improve perceptual ability and cause neural rewiring in the brain. This wave of research challenges demand to better understand some of core research questions include "how does the brain change with learning (online insight)?" and "how does it change after learning (offline insight)?".

Addressing these central questions would allow developing new and more effective interventions regarding individual variability in learning and is going to enable the next great advances in neuroscience.

This dissertation aims to present both "online" and "offline" insights of the neural mechanisms underlying visual perceptual learning (VPL) by obtaining resting-state functional magnetic resonance imaging (fMRI) scans of human brains before and after a task fMRI session involving visual perceptual training. During the task-fMRI session, participants performed a motion discrimination task in which they judged the direction of moving dots with a coherence level that varied between trials. The main results include (i) examining neural activations during "online" training, (ii) neural activations changes between two separate days, (iii) functional connectivity change before and after task and, (iv) relationship between resting-state functional connectivity changes and VPL after training. Here, we suggest that around 20 minutes of perceptual training induces plastic changes in offline functional connectivity specifically in brain regions representing the trained visual feature. Further our results emphasized the distinct roles of feature-representation regions and decision-related regions in VPL.

TABLE OF CONTENTS

LIST OF FIGURES

LIST OF TABLES

ACKNOWLEDGEMENTS

DEDICATION

To my dear parents and husband for their unconditional love and support during this
arduous journey

Chapter 1

TERMINOLOGY

Less than three decades ago it was believed that after about puberty the human brain could not change and by the time it has become hard-wired and fixed [59]. However great amounts of studies showed that the brain never stops changing and in fact reorganizes itself through learning. Another misconception about the brain was that we only use parts of it at any given time and it is silent when we do nothing. It is found by research studies that even when we are at a rest and thinking of nothing, our brain is highly active. Advances in technology, such as Magnetic Resonance Imaging (MRI) and functional MRI (fMRI) paved the path for scientists to make aforementioned important discoveries. One of these interesting discoveries is that every time we learn a skill, we change our brain which has become a great frontier in neuroscience to understand the human brain. This chapter is organized introduce some of the main terminologies relevant to "how do we learn?" and "how does the brain change with learning?"

1.1   Neuroplasticity

Learning is the ability to acquire new knowledge or skills through instruction or experience and that the capacity of the brain to change with experience and learning is called brain plasticity or neuroplasticity [1, 3]. According to prior studies the brain can change in three very basic ways to support learning [59], including (a) chemical changes (b) structural changes and, and (c) functional changes (see Fig 1 and Fig 2).

(a) Chemical changes

The brain functions by transferring chemicals signals between brain cells, which is called neurons. To support learning, the brain can increase the concentrations of these chemical signaling that is taking place between neurons (see Fig 1). Because this change can happen rapidly, this supports short-term improvement in the performance of a skill or memory.
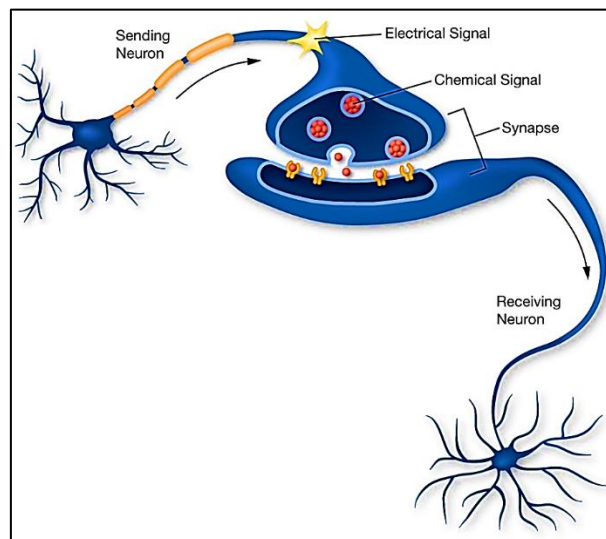
Figure 1. Neurons communication.
Information from one neuron flows to another neuron across a small gap called a synapse.
At the synapse, electrical signals are translated into chemical signals in order to
cross the gap [60].

(b) Structural changes

The second way that the brain can change to support learning is by altering its structure. Here the physical structure of the brain is changing and this takes a bit more time. These type of changes are related to long-term improvement in a skill or memory. A remarkable example of this type of plasticity is the study that showed London taxi drivers have a larger hippocampus than London bus drivers. It is because taxi drivers have to memorize a map of London in order to navigate around London whereas bus drivers follow a limited set of routes.

(c) Functional changes

The third way that the brain can change to support learning is by altering its function. As a brain region is getting used it becomes more and more excitable and easier for the brain to use it again and travel its pathway. Brain includes these areas that increase their excitability, accordingly the brain shifts how and when they are activated. With learning, whole networks of brain activity are shifting and changing. So neuroplasticity is supported by chemical, by structural, and by functional changes, and these are happening across the whole brain. They can occur in isolation from one or another, but most often, they take place in concert. Together, they support learning and they're taking place all the time.
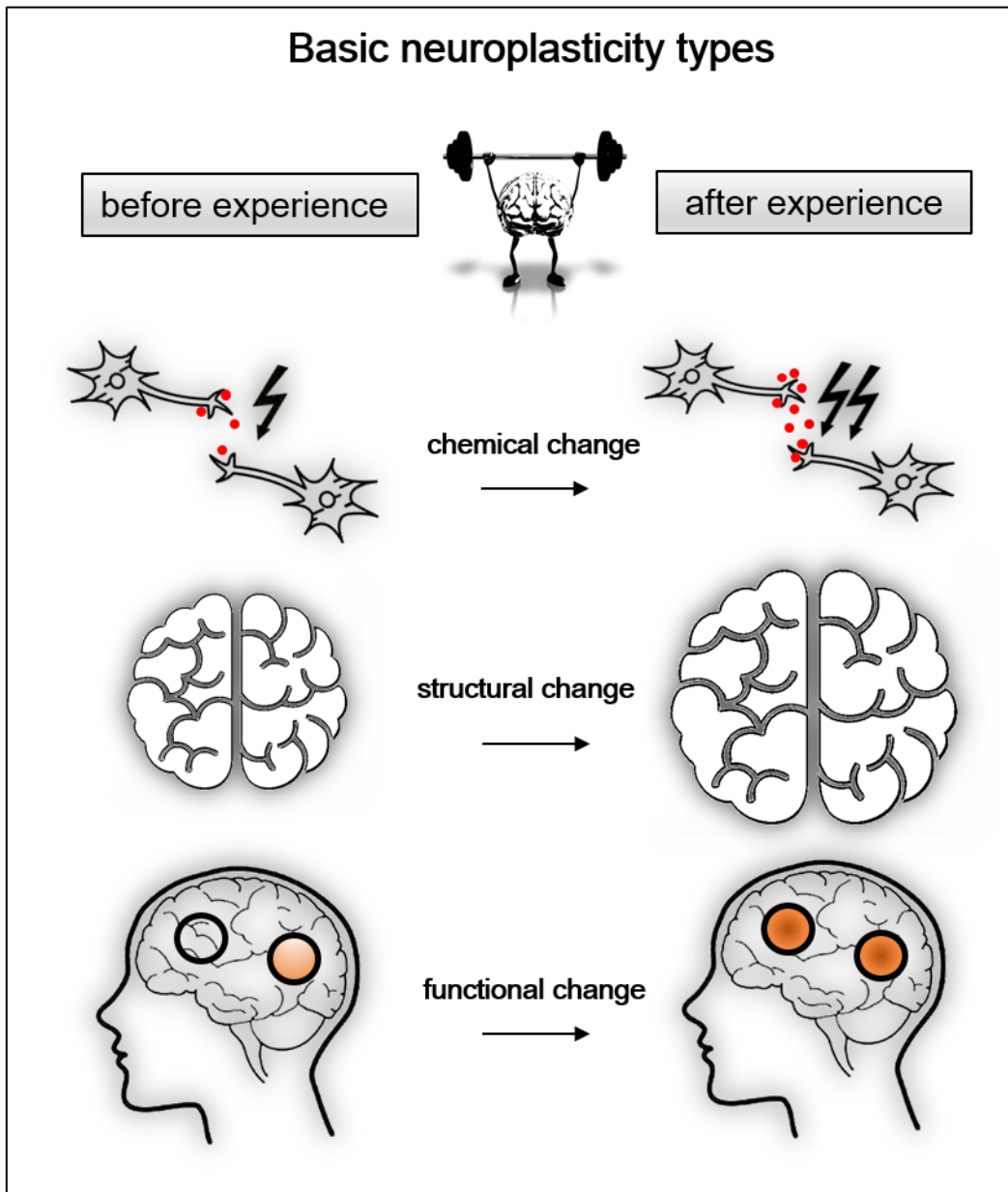
Figure 2. Neuroplasticity Types.
Schematic illustration of chemical, structural and functional changes occurs in the brain as the effect of learning.

1.2 Learning

Learning means the degree to adapting to the environment and responding to changes in it. It also refers to the process by which experiences change the nervous system and the behavior. Learning can take at least four basic forms: *perceptual learning*, *stimulus-response learning*, *motor learning*, and *relational learning* [63]. The main focus of the current thesis is on perceptual learning per se.

What is perceptual learning?

The ability to recognize stimuli that have been perceived before is called perceptual learning. It can involve learning to recognize entirely new stimuli, or it can involve learning to recognize changes or variations in familiar stimuli [3].
Perceptual learning and neuroplasticity have been studied in all the sensory modalities including vision, hearing, and touch perception [61, 62] and primarily accomplished by changes in the sensory association cortex. The focus of the current thesis is on vision modality per se.

1.3 Visual Perceptual Learning

Repeated exposure to a specific visual feature improves perceptual sensitivity and behavioural accuracy to the trained feature [1–3]. This process is known as visual perceptual learning (VPL), and is considered an effective tool for exploring experience-dependent plasticity in the brain [4–6]. For example, radiologists can identify a tumor from the pattern of spots on an X-ray scan easily, jewelers routinely classify diamonds that appear very similar to the uninitiated into different grades with high precision, whereas it is impossible for an untrained person to perform these skills. Such feats are possible because the experts' eyes are trained through practice and experience.

Therefore, VPL is regarded as an important tool that can help to clarify the mechanisms of adult visual and brain plasticity.

1.4   Models of Visual Perceptual learning

Visual processing consists of many different stages leading from eyes to cortical areas for cognitive processes such as decision making (see Fig 3). It is unlikely that all types of visual perceptual learning sharing common cortical stages. The stages in which one type of visual perceptual learning occurs may depend on many factors, including the learned visual feature such as orientation and contrast, the type of tasks such as a detection task or a discrimination task, and exposure to a feature without a task [3,4]. For instance, some types of visual perceptual learning may only involve lower stages of visual processing, such as V1, while other types of visual perceptual learning may involve multiple stages of visual processing. Models of different mechanisms are proposed depending on the stages [66]. The following three models fit well with different types of perceptual learning that take place in different stages of the visual processing stream.

(a) *Early stage, local network model*:

In this model, the neural reorganization due to perceptual learning can occur in a low-level cortex, including the primary visual cortex (V1), which is the first visual cortex onto which visual signals are projected [4,64,65]. This model indicates the mechanism of a type of perceptual learning that can involve only one level of visual processing and suggests that perceptual learning does not necessarily require lower-to-higher or higher-to lower connections between different cortical areas at different stages of visual processing (see Fig 3).

(b) *Mid-level stage, reweighting*:

In this model [67], learning occurs by changing the strength (reweighting) of neural connections between the early visual stages, such as V1, in which highly local processing occurs, and a decision unit. The changes occur in the neural connections specifically for a given task. In this sense, it is possible that different stages between the earliest visual stage and the decision unit are involved (see Fig 3).

(c) *Higher-to-lower stages*:

This model is based on reverse hierarchy theory (RHT) indicates that learning is an attention guided process [66, 68]. According to this model, visual learning begins at high-level visual areas that may be able to deal with a task requiring discriminating signals with large differences (see Fig 3). When a task requires discrimination of signals with smaller differences, the site of learning proceeds to lower visual areas where signals with smaller differences can be discriminated. RHT indicates that learning is driven by the attention that selects neuronal population suitable for the levels of the signal.
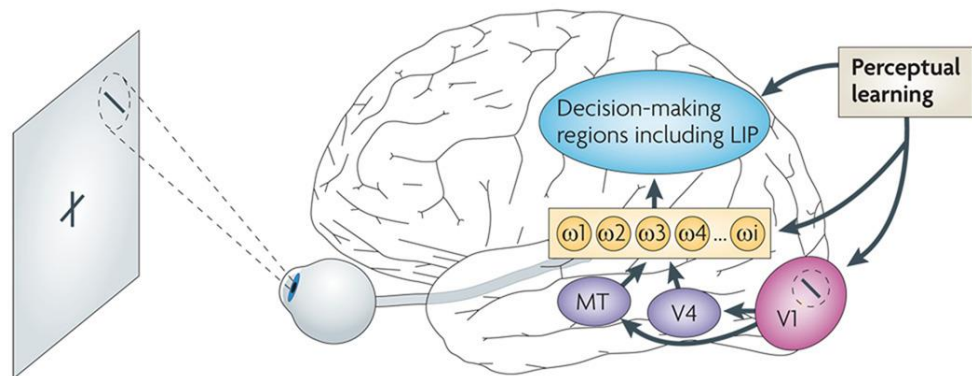
Figure 3. **Neural correlates of VPL.**

The regions of the brain thought to be altered by visual perceptual learning (VPL). Some experiments have indicated that training on a visual task changes visual representations in the early stages of visual signal processing. Others have instead suggested that training alters the weight of connections (ω1, ω2 ... ωi) between the visual cortex and regions of the brain involved in decision making, or within the decision-making regions themselves. The figure is taken from Sasaki et al. 2010 [4].

1.5   Major directions in VPL research

Mainly, VPL research has three major divergent directions [4], Specificity versus generalization, Lower versus higher brain locus and task-relevant versus task-irrelevant (TR-VPL and TI-VPL, respectively) [4].

1.5.1   Specificity versus generalization of VPL

The first direction compares the specificity and generalization divergence view of VPL. Seminal psychophysical studies reported that improvement in visual performance is largely specific to stimulus features such as retinal location, contrast orientation spatial frequency, motion direction, or background texture that are trained or exposed during training. In other words, VPL is not generalized to other features. Such high specificity of VPL has been often regarded as the evidence for refinement of the neural representation of a trained visual feature.

However, recent studies have indicated that under some conditions VPL can be generalized to untrained features. The recent VPL studies that reported generalization of VPL to untrained features under certain conditions. These results support the view that VPL is mostly caused by higher-level cognitive factors such as enduring attentional inhibition of the untrained features, selective reweighting of readout process to find specific visual representations which are the most useful for a trained task.

1.5.2   Lower versus higher brain locus of VPL

The second direction of studies has suggested that VPL is associated with changes primarily in visual areas (visual model), while the other line of studies has proposed that VPL emerges from changes in higher-level cognitive areas that are involved in decision making or changes in weighting between the visual and cognitive areas (cognitive model).
The accumulated findings can be generally framed in terms of one of two opposing models: the visual and cognitive models. Both models have concentrated substantial psychophysical, physiological, and computational findings in their respective favors.

1.5.3   TR-VPL versus TI-VPL

Third direction concerns, whether task-relevant and task-irrelevant VPL share a common mechanism or reflect distinct mechanisms. TR-VPL of a feature happens to training on a task of the visual feature and is gated by focused attention to the feature in principle. On the other hand, TI-VPL is defined as VPL of a feature that is irrelevant to a given task. It has been found that TI-VPL does not necessarily require attention to, and awareness of, the trained feature. Some studies have suggested that the same or similar mechanisms underlie TI-VPL and TR-VPL, while others have suggested distinct mechanisms.

1.6   Resting-State Functional Connectivity

When one performs a specific cognitive task that involves attention or reflection, the brain only uses 5% of its total metabolic expenditure [18]. Yet, how does the brain expend the majority of its energy? In 1995, Biswal [18] and colleagues observed that regions that are co-activated during a task are correlated with their activity in the absence of a task. This observation led to the conclusion that intrinsic activity in the brain is a major source of energy expenditure.

Spontaneous fluctuations involve the low-frequency (LF: <0.1 Hz) that can be measured indirectly using blood oxygen level-dependent (BOLD) functional magnetic resonance imaging (fMRI). These BOLD signals across brain regions are known as resting-state functional connectivity (rs-FC). Previously, spontaneous low-frequency BOLD fluctuations were discarded as noise in task-based fMRI studies. These signals were considered to be crucial to understanding the intrinsic activity of the brain.
Resting-state BOLD correlations are observed when subjects are instructed to relax inside the MRI scanner without engaging in a specific task. Temporal correlations do not appear to be random because patterns of connectivity have been reliably identified across studies and subjects.

Resting-state functional connectivity analysis has largely enabled scientists to measure task-free (offline) changes and experience-dependent plasticity in the human brain which has become a great frontier in the understanding of offline mechanisms of human brain and in VPL as well.

Chapter 2

INTRODUCTION

2.1   Research Background

Previous studies using functional magnetic resonance imaging (fMRI) in humans have revealed that different brain regions contribute to VPL in distinct ways, depending on their specialized roles [7,8]. These studies have typically examined how brain activation to specific visual stimuli changes over the course of perceptual training. For instance, several studies have shown that stimulus-induced activation in brain regions representing specific visual features (e.g., the early visual cortex) tends to increase after intensive perceptual training [2,9], whereas activation in regions related to higher-order cognitive processes tends to decrease after training [9]. Other studies have reported refinements in neural representations of trained visual features after VPL, indicating training-induced plasticity in feature-representation regions [5,8]. While these findings have provided useful insights into the "online" processes supporting VPL, it is also known that "offline" processes after task completion (e.g., consolidation during sleep) play critical roles [10,11]. However, because the majority of existing fMRI studies have exclusively investigated brain activation during task periods, the contribution of offline mechanisms to VPL remains to be elucidated. The importance of post-task offline processes in VPL has typically been studied by focusing on sleep-related consolidation processes [11,12]. However, recent studies have also highlighted the importance of wakeful resting periods immediately after training [13–15]. Neuroimaging studies utilizing resting-state functional connectivity (rs-FC) [16–18] are particularly useful for investigating experience-dependent reorganization in the brain after performing cognitive tasks. Evidence from diverse domains of cognitive neuroscience research has suggested that

post-task rs-FC changes reflect recent visual/cognitive experiences [14,19], and further predict the subsequent performance of memory and learning [15,20]. Studies of episodic memory are notable examples, showing that rs-FC between category-selective regions (e.g., the fusiform face area) and memory-related regions (e.g., the hippocampus) during wakeful rest immediately after performing encoding tasks is predictive of subsequent memory performance [13,21]. Although VPL and episodic memory formation are supported by different neural substrates, both involve experience-induced plasticity as underlying mechanisms [10,22,23]. This raises the possibility that rs-FC during wakeful rest immediately after training may also play a key role in VPL.

2.2   Research Issues and Existing Gap

Only a few studies have investigated training-induced rs-FC changes after VPL, and the results have been mixed. One study examined rs-FC before and after intensive training on a visual shape discrimination task, finding that rs-FC between the visual feature representation region (i.e., V3) and the dorsal attention system (e.g., the frontal eye field and superior parietal lobule) decreased after training [24]. However, this study investigated the effects of intensive training over several days (2–9 days) and did not examine rs-FC changes in the early learning phase. In contrast, another fMRI study used visual motion discrimination training with a much shorter timescale (~90 min), finding that rs-FC between the hippocampus and striatum increased during a wakeful rest period immediately after training [25]. While this study revealed rapid reorganization of rs-FC after a brief period of perceptual training, no rs-FC changes were detected in the visual feature representation region, unlike the earlier study. Thus, it remains unclear whether visual feature representation regions show training-induced rs-FC changes immediately after training.

2.3   The Current Study

In the current fMRI study, we examined whether a brief period of visual perceptual training-induced rapid reorganization of rs-FC changes immediately after training in the visual feature representation regions. Participants were trained on a visual motion discrimination task for a short period (~30 min), in which they judged the direction of coherently moving dots randomly chosen from three coherence levels (20, 40 and 80%). We localized the MT+, a brain region representing visual motion [26–33], by analyzing the parametric effects of motion coherence on stimulus-induced activation during the task fMRI (t-fMRI) session. Importantly, we obtained resting-state fMRI (rs-fMRI) scans before and immediately after the task to examine whether a brief period of visual motion discrimination training induces rs-FC changes with the MT+. Furthermore, we examined whether training-induced rs-FC changes immediately after training were associated with subsequent performance improvement. This question was inspired by recent reports that experience-induced rs-FC changes shortly after memory encoding tasks predict subsequent memory performance in later periods (~24 hours) [21]. To examine this issue, we invited the same participants back on the second day of the experiment to perform the motion discrimination task in the scanner.

Chapter 3

MATERIALS AND METHODS

This chapter provides the study experimental design protocol, parameters and neuroimaging data pre- and post-processing steps in detail.

3.1   Participants

Twenty-one healthy right-handed participants with normal or corrected-to-normal vision were recruited for the experiment. All participants were native Japanese speakers with no history of neuropsychiatric disorders or current use of psychoactive medications. All participants provided written informed consent according to guidelines approved by the institutional review board of Kochi University of Technology. Participants received 1000 yen per hour for participation. One participant was excluded due to being scanned on day 2 after 30 days from day 1 experiment (see experimental protocol), while all other participants were scanned on day 2 after 1 or 2 days apart (see Fig 4). Thus, the data from 20 participants (mean age 18.6 years, range 18–21; eight females) were analyzed and reported in the study.

3.2 Experimental Procedure

3.2.1 Session Procedure

The experiment was conducted in four stages over 2 days (day 1 and 2). On day 1, participants were scanned during three consecutive stages: started with pre-task resting-state functional magnetic resonance imaging (rs-fMRI) followed by task-fMRI (t-fMRI) and completed with post-task rs-fMRI. On day 2, the same participants underwent the second t-fMRI session with the same task settings used for day 1.

3.2.2 Task design

In each t-fMRI session, participants performed six runs of a visual motion discrimination task, in which they judged the direction of random-dot motion (see Fig 5). Randomly moving dots were presented with three coherence levels (20, 40 and 80%) and with two directions (upward and downward). Participants discriminated which of the two directions the majority of dots were moving in, by pressing one of two target buttons. Assignments of the target buttons to the motion directions were counterbalanced across participants (left and right buttons are assigned to upward and downward motion respectively, and vice versa). The target button assignment for each participant was constant for two separate t-fMRI sessions. The presentation order of the stimuli (three coherence levels and two directions) was pseudorandomized. Each run consisted of 70 trials. The first and last five trials in each run were presented with the highest coherence level (80%) and were excluded from data analysis. Thus, the middle 60 trials (20 trials for each coherence level) were included in our analysis. Participants performed a total of 360 (6×60) effective trials on each t-fMRI session.

16

3.2.3 *Single trial design*

Each trial began with a 750-ms presentation of a red fixation cross-cueing the subsequent stimulus comprised of coherently moving dots for 300 ms. The color of the fixation cross became white when the dot stimuli disappeared, and remained white for 1750 ms (see Fig 6). Participants were required to press the corresponding button with their right thumb as quickly and accurately as possible within a response window of 1050 ms (see Fig 6). The onset of the response window was matched to the timing of the dot stimuli presentation. In rs-fMRI sessions, all participants were scanned for 5 minutes and 20 seconds before and after t-fMRI on day 1. The following instructions were given to the participants: please rest with your eyes open, and remain calm.
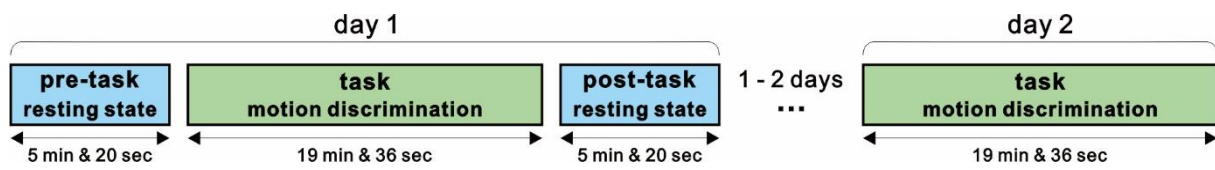
Figure 4. **Experimental procedure**
Experiments were conducted over 2 days: day 1 and day 2. On day 1, fMRI scanning started with pre-task resting-state scans, followed by motion discrimination task scans, and post-task resting-state scans. On day 2, the same motion discrimination task was administered in the scanner
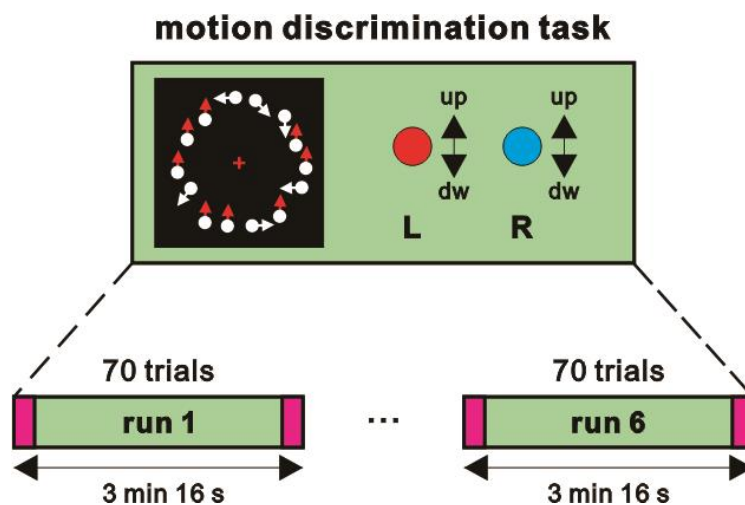
Figure 5. **Motion discrimination task**.
In each task-fMRI session (day 1 and 2), participants performed six runs of the motion discrimination task. The coherence level (20, 40, or 80%) and motion direction (upward or downward) varied from trial to trial. Participants were required to press the corresponding button with their right thumb as quickly and accurately as possible within a response window of 1050 ms.
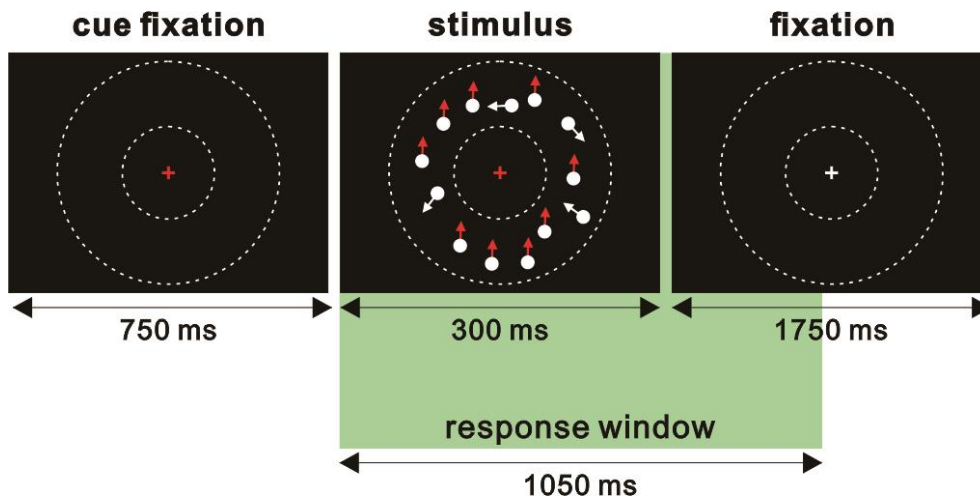
Figure 6. A sample single trial.
Each trial of the motion discrimination task began with 750-ms presentation of a red fixation cross-cueing a subsequent visual stimulus comprised of coherently moving dots for 300 ms. The color of the fixation cross became white when the dot stimuli disappeared and remained white for 1750 ms. Participants were asked to respond within a response window of 1050 ms.

3.2.3 Stimuli

All stimuli were generated in MATLAB version 2012a, using the Psychophysics Toolbox extension, version 3.0.10 [34,35]. The stimuli were similar to those used in a previous study of perceptual decision-making [8,36] Each motion stimulus was composed of 150 white dots moving inside a donut-shaped display patch with a white cross in the center of the patch, on a black background (see Fig 6). The display patch and cross were centered on the screen and extended from 6 to 12° of visual angle. Within the display patch, every dot moved at the speed of 10° of visual angle per second. Some dots moved coherently in one direction, while others moved randomly. The percentage of coherently moving dots determined the coherence, which was presented with three levels (20, 40, and 80%). Dot presentation was controlled to remove local motion signals following a standard method for generating motion stimuli [27,28,37,38]. Specifically, upon stimulus onset, the dots were presented at new random locations on each of first three frames. They were relocated after two subsequent frames so that the dots in frame 1 were repositioned in frame 4, and the dots in frame 2 were repositioned in frame 5, and so on. When repositioned, each dot was either randomly presented at the new location or aligned with the pre-determined motion direction (upward or downward), depending on the pre-determined motion strength on that trial. Each stimulus was composed of 18 video frames with 60 Hz refresh rates (i.e., 300-ms presentation).

3.3 fMRI Scanning

Participants were scanned with a 3T Siemens Verio MRI scanner with a 32-channel head coil to obtain anatomical and functional scans. High-resolution anatomical images were acquired from each participant on day 1 after the second resting scan with a magnetisation-prepared rapid acquisition gradient echo (MPRAGE) T1-weighted sequence (repetition time (TR) 2500 ms; echo time (TE) 4.32 ms; flip angle (FA) 8°; 192 slices; slice thickness 1 mm, in-plane resolution 0.9×0.9 mm^2). Functional images were acquired using a multi-band acceleration echo-planar imaging sequence (TR 0.8 sec; TE 30 ms; FA 45°; 80 slices in interleaved order; slice thickness 2 mm; in-plane resolution 3×3 mm^2; multiband factor 8). Each functional run during the motion discrimination task involved 245 volumes,

and each resting-state acquisition involved 400 volumes. The first 10 volumes of all functional runs (task and rest) were discarded to allow for T1 equilibration of longitudinal magnetization.

3.4   fMRI Preprocessing

Functional data were analyzed using SPM12 (http://fil.ion.ucl.ac.uk/spm/software/spm12). Preprocessing of functional images (both resting scans and task scans) involved sequential realignment across volumes and runs, coregistration of functional images to anatomical images, spatial normalisation to a standard MNI template with normalisation parameters estimated for the anatomical scans, spatial smoothing with a 8-mm full-width at half-maximum (FWHM) Gaussian kernel, and resampling into 1-mm isotropic voxels. No global signal regression was performed. Due to imaging, short TR slice time correction was not applied to the data. Table 1 shows the fMRI pre and post processing in detail.

3.5   General linear model

3.5.1   *First-level analysis*

A general linear model (GLM) [39] approach was used to estimate parameter values for task events. In the t-fMRI analysis, the effect of interest was the influence of changing coherence levels of visual motion from trial to trial. The trials with upward motion and those with downward motion were modeled with separate regressors, each of which was modulated by the parametric effect of mean-centered coherence levels across trials. Trials in which participants did not make a button press were separately coded in the GLM as nuisance effects. Those task events were time-locked to the stimulus onset of each trial, then convolved with canonical hemodynamic response function (HRF) implemented in SPM. Additionally, six motion parameters (three translation and three rotation parameters per frame), as well as white matter (WM) and cerebrospinal fluid (CSF) signal time series, were also included in GLM as nuisance effects.

Parameters were then estimated for each voxel across the whole brain. In the rs-fMRI analysis, time series were extracted from 5-mm radius spheres centered on individual seed coordinates (the MT+, dACC and bilateral insula) after regressing out the eight nuisance variables (i.e., six motion parameters, WM and CSF signal time series). The extracted seed time series was then band-pass filtered between 0.01 Hz to 0.1 Hz to reduce the effects of low-frequency drift and high-frequency noise [13,25,40]. Finally, a separate GLM was estimated for each seed, which included the seed time series as the regressor of interest in addition to the eight nuisance variables.

3.5.2   Second-level analysis

Maps of parameter estimates were first contrasted with individual participants.   The contrast maps were collected from all participants and were subjected to a group-mean one-sample t-test based on permutation methods (5000 permutations) implemented in *randomize* in FSL suite (http://fmrib.ox.ac.uk/fsl/).   Then voxel clusters were identified using a voxel-wise uncorrected threshold of $P < .001$.   The voxel clusters were tested for a significance with a threshold of $P < 0.05$ corrected by family-wise error (FWE) rate.   The peaks of significant clusters were then identified and listed on tables.   If multiple peaks were identified within 12 mm, the most significant peak was kept.

Table 1 fMRI Pre- and post-processing steps

fMRI Analyses Steps

Preprocessing	First-level (task)	First-level (rest)	Second-level
• SPM12	• GLM	• GLM	• FSL
• Realignment	• Regressors (13)	• Regressors	• Group-mean
• Coregistration			• 1-sample t-test
• Normalization	• Upward	• 6-MP	• Permutation
• Smoothing	• Downward	• WM	• Randomise
	• Parametric-up	• CSF	• Clusters tested for FWE (p<0.05)
	• Parametric-down	• Seed TC (5mm-radius)	
	• error	• Bandpass (0.01–0.1hz)	
	• 6-MP	• Separate GLM/seed	
	• WM	• 8-nuisance	
	• CSF		

3.6   Brain-behavior correlation analysis

To compute training-induced rs-FC changes between specific pairs of regions, we used a method following Tambini *et al*. (2010) [13]. First, fMRI time series were extracted from a 5-mm radius sphere centered on the peak coordinates of each of the regions identified by the rs-FC analysis with the MT+ seed (Post-task vs. Pre-task rest), after regressing out the eight nuisance variables (six motion parameters and WM/CSF signal time series). Next, Pearson correlation coefficients between the two-time series (the MT+ and each region of interest) were calculated, and subsequently, Fisher Z transformed. The difference in Z (Post-task minus Pre-task) was used as an individual participant's measure of training-induced rs-FC change. Finally, Pearson correlation coefficients between the training-induced rs-FC change and accuracy change were computed across participants. Distributions of variables (behavioral and rs-FC changes) were not significantly different from a normal distribution (Lilliefors test, $P > 0.062$).

Chapter 4

RESULTS

4.1 Behavioral results

To assess behavioural improvement after visual perceptual training, participants' discrimination accuracy and reaction time for coherently moving dots were compared between the 2 days of t-fMRI sessions (day 1 and 2). Participants showed a marginally significant increase in overall discrimination accuracy (day 1: 83.8 ± 8.0%, mean ± standard deviation; day 2: 86.8 ± 5.8%; paired t test, $t(19) = 1.95$, $P = 0.066$; Cohen's $d_{av} = 0.43$) [41] and a significant decrease in overall discrimination reaction time (day 1: 696 ± 70 ms; day 2: 665 ± 72 ms; paired t test, $t(19) = 3.17$, $P = 0.005$; Cohen's $d_{av} = 0.43$), (see Fig 7). These results confirmed that a single session of brief visual perceptual training (~30 min) induced behavioural improvement that lasted over 24 hours. Behavioural improvement further assessed during day 1 runs. Run-specific behavioural measures such as accuracy, reaction time and Inverse Efficiency (IE) were calculated for 6 runs in day 1 separately. An analysis of variance did not show significant effect of accuracy, reaction time and IE across 6 runs of the day 1 (accuracy: $F(5,114) = 0.29$, $P = 0.91$; reaction time: $F(5,114) = 0.56$, $P = 0.73$, IE: $F(5,114) = 0.21$, $P = 0.96$). Additional comparisons were conducted between first (run 1) and last (run 6) runs in day 1. Participants did not show significant improvement from run 1 to run 6 (ACC: paired t test, $t(19) = 1.14$, $P = 0.268$; RT: paired t test, $t(19) = 1.09$, $P = 0.29$; IE: paired t test, $t(19) = 0.30$, $P = 0.76$), (see Table 2).
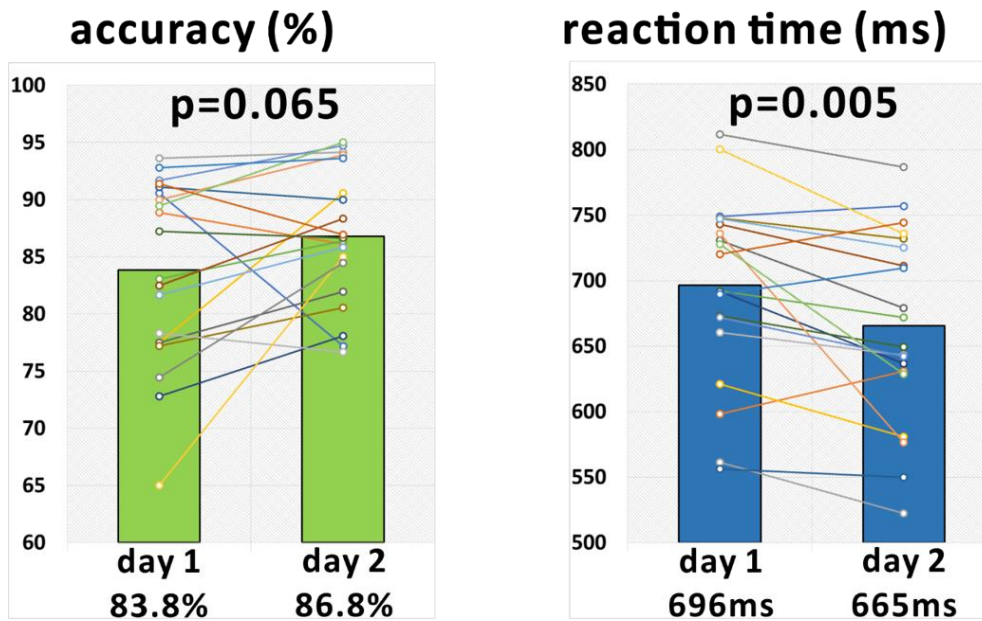
Figure 7. Behavioral results.
The left panel shows subjects performed motion discrimination task more accurately (left panel) and faster (right panel) in day2.

Table 2. Session-wise behavioral measures (6 runs of day 1)

	run 1	run 2	run 3	run 4	run 5	run 6
ACC(%)	84.4 (6.4)	85.6 (8.8)	84.3 (10.6)	83.6 (12.5)	82.5 (9.1)	82.7 (9.4)
RT(ms)	586 (71)	594 (61)	594 (61)	576 (72)	567 (82)	570 (78)
IE(ms)	7.0 (0.9)	7.0 (0.7)	7.1 (0.8)	7.0 (0.8)	6.9 (0.7)	6.9 (0.8)

4.2   Task-related fMRI activation

To identify brain regions involved in visual motion discrimination, we examined stimulus-induced fMRI activation that was parametrically modulated by the coherence level of moving dots. First, we combined t-fMRI data from both sessions (day 1 and 2) to probe stimulus-induced activation. As predicted, we found that stimulus-induced activation was positively modulated by the coherence level in the MT+, a region that is well established as the feature-representation region for visual motion ($P < 0.05$, cluster-level FWE corrected; see Fig 8A and Table 3). The peak MNI coordinates of the MT+ ($x = 42$, $y = -64$, $z = 6$) were close to those reported in previous studies [8,42,43]. On the other hand, stimulus-induced activation was negatively modulated by the coherence level in the dorsal anterior cingulate cortex (dACC) and bilateral insula (see Fig 8A), the regions known to show task-difficulty dependent activation during perceptual decision-making tasks [44,45]. Next, we examined whether these regions showed learning-dependent activation changes between day 1 and day 2. For this analysis, we extracted the parametric effects of coherence level from these regions separately for day 1 and day 2 (see Fig 8B). No region showed a significant difference in the parametric effect of the coherence level between day 1 and day 2 ($t(19) < 0.90$, $P > 0.382$). Note that we used orthogonal contrasts for localizations of the regions (day 1 and 2, combined) and comparisons of activation (day 1 vs. day 2), thereby avoiding circular analysis. Run-specific learning-dependent activation changes further assessed on day 1 runs.

We extracted the parametric effects of coherence level from the regions (MT+,dACC, and bilateral insula) separately for each run of day 1. No region showed significant difference in the parametric effect of the coherence level across day 1 runs (MT: $F(5,114) = 1$, $P = 0.38$; left insula: $F(5,114) = 1.52$, $P = 0.19$, right insula: $F(5,114) = 1.27$, $P = 0.28$; dACC: $F(5,114) = 0.65$, $P = 0.66$). Additional comparisons between first and last runs of day 1 of the parametric activation of the regions (MT+,dACC, and bilateral insula), also did not show significant improvement from run 1 to run 6 (MT: paired t test, $t(19) = 0.64$, $P = 0.52$; left insula: paired t test, $t(19) = -0.17$, $P = 0.86$; right insula: paired t test, $t(19) = -1.05$, $P = 0.30$; dACC: paired t test, $t(19) = 0.17$, $P = 0.86$).
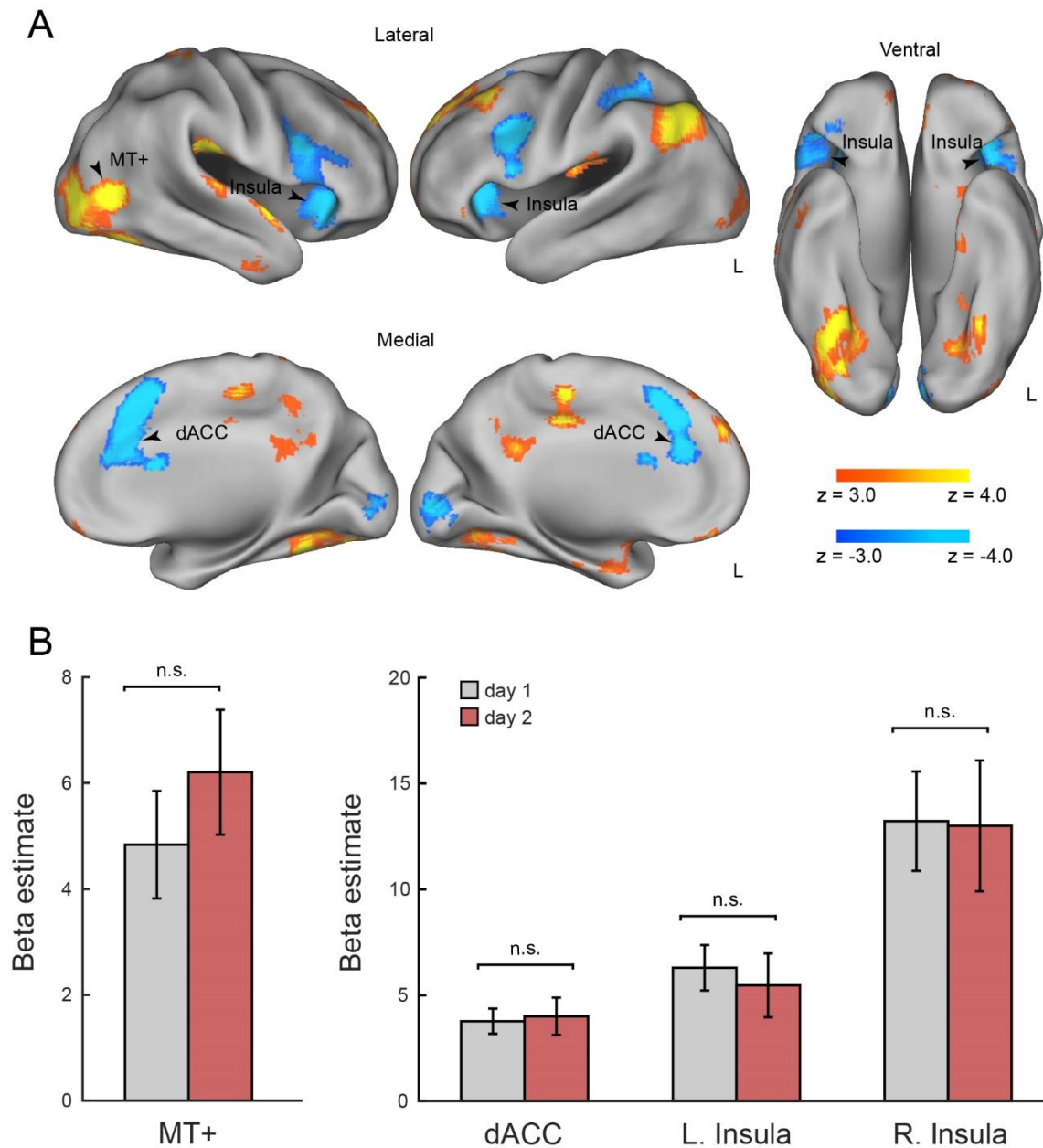
Figure 8. Task-related fMRI activation.
(A) Positive and negative parametric effects of motion coherence. The statistical maps indicate brain regions showing significant activation increases with the coherence level (hot, including the MT+) and decreases with the coherence level (cold, including the dACC and bilateral insula). All maps are thresholded at $P < 0.05$, cluster-level FWE corrected across the whole brain. (B) Mean beta values for regions MT+, dACC, left and right insula. Peak coordinates derived from combining day 1 and day 2 task-fMRI data.

Table 3. Activation by the parametric effect of motion coherence
Regions showing significant activation by the parametric effect of motion coherence during the performance of direction discrimination task (cluster-level FWE-corrected $P < 0.05$).

Region	Hemi	#voxels	MNI coordinates			Peak t
			x	y	z	
Positive parametric effect						
Frontal pole	R	2758	16	50	40	7.32
Temporal occipital fusiform cortex	R	2379	26	−52	−18	7.72
Lateral occipital cortex (MT+)	R		42	−64	6	7.59
Lateral occipital cortex	L	1525	−44	−64	42	8.89
Parietal operculum cortex	R	797	46	−24	22	7.87
Precuneus cortex	R	765	0	−54	32	5.78
Cingulate gyrus	L	668	−4	−28	42	7.48
Putamen[*]	L	575	−30	−16	2	6.07
Temporal occipital fusiform cortex	L	453	−30	−58	−14	5.68
Superior parietal lobule	R	334	18	−46	70	5.25
Parietal operculum cortex	L	329	−40	−28	20	5.64
Middle temporal gyrus	R	270	58	−8	−28	5.35
Lateral occipital cortex	L	248	−38	−84	−10	4.45
Frontal medial cortex	L	212	−2	46	−18	5.24
Insular cortex/putamen[*]	R	208	32	−16	4	5.21
Superior temporal gyrus	R	193	58	0	−4	5.42
Negative parametric effect						
Paracingulate gyrus (dACC)	R	2559	16	22	32	7.83
Insular cortex	R	1945	36	22	0	7.41
Insular cortex	L	1748	−26	20	2	7.41
Supramarginal gyrus	L	617	−32	−38	34	5.25
Occipital pole	R	533	−6	−92	−2	6.09

Anatomical labels derived from Harvard-Oxford cortical structural atlas. [*]Labels derived from Harvard-Oxford Subcortical structural atlas. L= left hemisphere, R = right hemisphere, #voxels = number of voxels. The MT+ was identified as the second peak of the cluster.

4.3   Resting-state functional connectivity

To examine training-induced changes in rs-FC, we contrasted seed-based functional connectivity during the pre-task and post-task rs-fMRI sessions. In this analysis, we selected the MT+ as the primary seed that was localized by the parametric effect of the coherence level on the day 1 t-fMRI session (MNI coordinates: $x = 42$ $y = -66$, $z = 8$). Note that we used only data from day 1 to avoid possible artifacts resulting from differences in head position between day 1 and day 2. First, we obtained rs-FC maps with the MT+ seed separately for the pre-task and post-task rs-fMRI sessions. This revealed that a greater number of voxels located across broad brain regions showed significant rs-FC with the MT+ during the post-task (relative to pre-task) rs-fMRI session (see Fig 9 and Fig 10). More specifically, we found prominent increases in rs-FC with the MT+ during the post-task (relative to pre-task) rs-fMRI session in the bilateral postcentral gyrus (POG), the left precentral gyrus (PrG), the left superior temporal gyrus (STG), the left middle temporal gyrus (MTG) and the lateral occipital cortex (LOC) ($P < 0.05$, cluster-level FWE corrected; see Fig 11 and Table 4). On the contrary, rs-FC with the MT+ was significantly decreased in subcortical regions (the thalamus and putamen) after the t-fMRI session (see Fig 11 and Table 4). Notably, we found no significant change in rs-FC between the pre- and post-task rs-fMRI sessions when we used the dACC, a task-difficulty dependent region, as a seed ($x = 14$, $y = 22$, $z = 34$; $P > 0.056$, cluster-level FWE corrected). Likewise, there were no significant rs-FC changes between the rs-fMRI sessions when we used the right and left insula as seeds (right: $x = 36$, $y = 22$, $z = 0$; $P > 0.052$, cluster-level FWE corrected; left: $x = -30$, $y = 30$, $z = 0$; $P > 0.202$, cluster-level FWE corrected). These findings suggest that the post-task rs-FC change occurred specifically in the brain regions representing the trained visual feature, but not in the task-difficulty dependent regions.
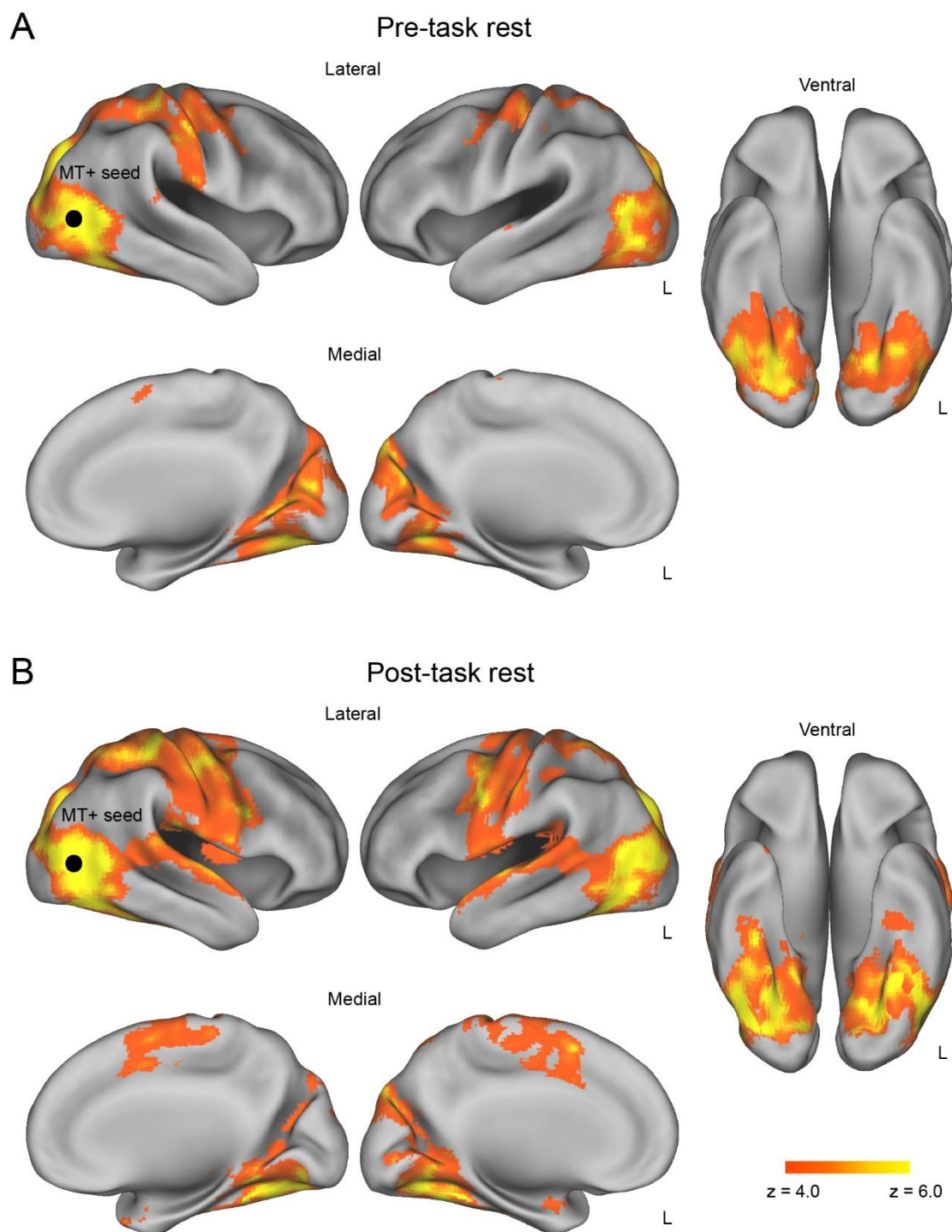
Figure 9. Resting-state functional connectivity with MT+ seed
(A) Pre-task rs-FC maps indicating areas that showed significant rs-FC with the MT+ before participants performed the motion discrimination task. (B) Post-task rs-FC maps indicating areas that showed significant rs-FC with the MT+ after participants performed the motion discrimination task. All maps are thresholded at P < 0.05, cluster-level FWE corrected across the whole brain.
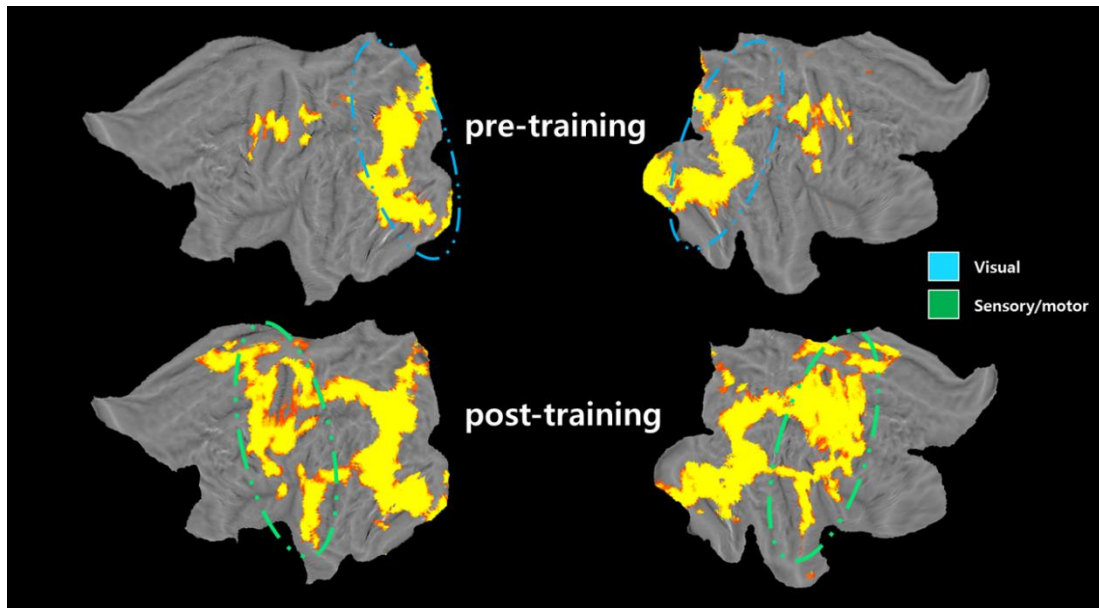
Figure 10. Resting-state functional connectivity with MT+ seed (flat view).
This figure illustrates the figure 9 in full-flat view. Green dotted-oval shapes show functional connectivity enhancement in post-training compared to pre-training resting state.
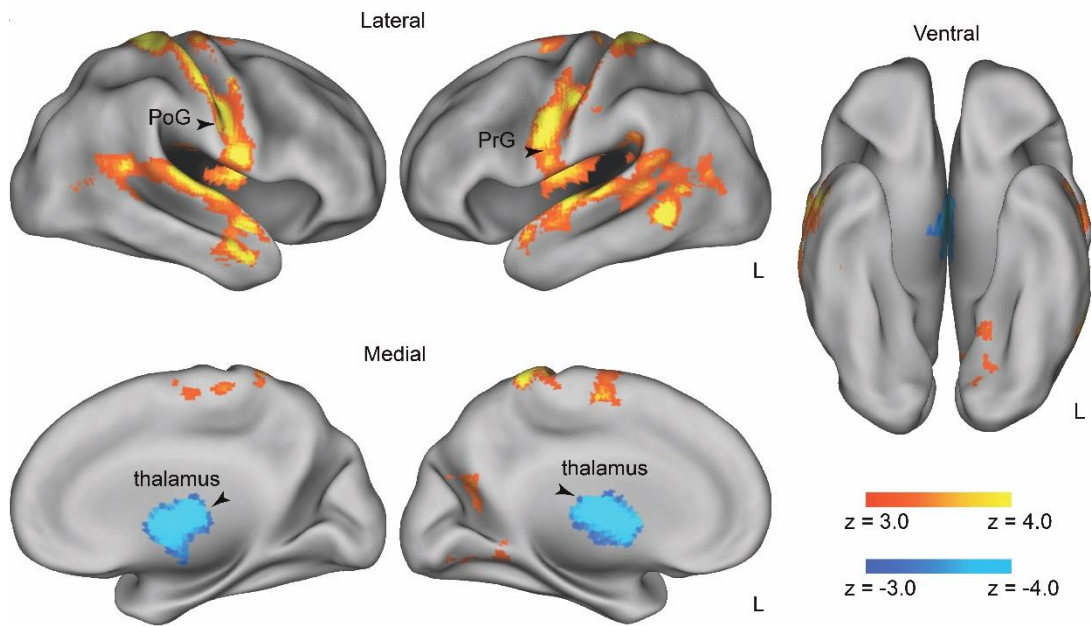
Figure 11. **Training-induced rs-FC changes**.
The statistical map indicates brain regions showing training-induced rs-FC changes with the MT+ seed (hot: Post-task > Pre-task rest, cold: Pre-task > Post-task rest). The arrowhead indicates the left PrG. All maps are thresholded at P < 0.05, cluster-level FWE corrected across the whole brain.

Table 4. Resting-state functional connectivity change with MT+
Regions showing significant rs-FC with the MT+ in pre-task rest, post-task rest, and contrasts of post-task > pre-task rest and pre-task > post-task rest (cluster-level FWE-corrected $P <$ 0.05). Subpeaks in a given cluster were listed if it survived at $P < 0.05$, voxel-wise FWE corrected across the whole brain.

Region	Hemi	#voxels	MNI coordinates x	y	z	Peak t
Pre-task rest						
Lateral occipital cortex	R	43483	44	−66	6	23.4
Precentral gyrus	L		−36	−22	56	10.7
Cerebellum[**]	L		−6	−72	−42	7.30
Postcentral gyrus	R		6	−36	66	6.97
Supramarginal gyrus	R		60	−36	14	6.77
Insular cortex	R		40	−2	12	6.67
Supplementary motor cortex	R	1136	6	2	58	6.56
Parietal operculum cortex	L	393	−42	−36	24	5.51
Post-task rest						
Lateral occipital cortex	R	70088	44	−66	6	21.1
Temporal pole	R		28	12	−30	8.69
Parahippocampal gyrus	L		−30	−6	−24	7.15
Parahippocampal gyrus	R		20	−2	−20	6.42
Amygdala[*]	R		30	−4	−24	6.2
Precentral gyrus	L		−36	8	20	6.19
Parahippocampal gyrus	R		22	2	−26	6.16
Intracalcarine cortex	R		4	−66	12	6
Thalamus[*]	R		20	−30	0	5.94
Post-task rest > Pre-task rest						
Postcentral gyrus	R	15884	22	−40	66	9.95
Postcentral gyrus	R		52	−12	50	9.6
Postcentral gyrus	L		−24	−40	68	8.19
Inferior temporal gyrus	L		−46	−46	−4	7.62
Middle temporal gyrus	L		−56	−54	−6	7.49
Superior temporal gyrus	L		−64	−16	2	6.72
Planum temporale	L		−52	−18	0	6.59
Superior frontal gyrus	L		−14	−4	60	6.45
Postcentral gyrus	R		40	−14	32	6.41
Middle temporal gyrus	R		52	2	−24	6.37
Precentral gyrus	L		−54	−4	24	6.32
Central opercular cortex	R		42	−12	14	6.27
Precuneous cortex	R	217	−10	−68	18	4.68
Pre-task rest > Post-task rest						
Thalamus[*]	L	2163	−6	−2	6	7.79
Thalamus[*]	L		−12	−22	14	7.59
Thalamus[*]	R		6	−16	12	7.04

Thalamus[*]	R	4	−4	6	6.75
Thalamus[*]	L	−16	−8	6	6.47
Thalamus[*]	R	20	−24	14	6.26
Putamen[*]	R	20	16	2	6.25

Anatomical labels derived from Harvard-Oxford cortical structural atlas. [*]Labels derived from Harvard-Oxford Subcortical structural atlas. [**]Labels derived from Automated Anatomical Labels. L= left hemisphere, R = right hemisphere, #voxels = number of voxels.

4.4 Brain-behavior correlation

We tested whether the training-induced rs-FC change in the MT+ predicts individuals' performance improvement (i.e., accuracy gain) on day 2. We found that accuracy gains were positively correlated with training-induced rs-FC changes between the MT+ and left PrG ($r = 0.522$, $P = 0.018$, uncorrected), indicating that ~27% of the inter-individual variation in accuracy gains was explained by the training-induced rs-FC change between these regions (Fig 12). However, given that we observed training-induced rs-FC change with the MT+ in 19 regions, the brain-behavior correlation in the left PrG did not survive multiple comparison corrections (see Table 5). We further tested whether the training-induced rs-FC change in the MT+ predicts individuals' performance improvement in reaction time (RT) and inverse efficiency (IE) on day 2 (see Tables 6 and 7). We found that only IE was negatively correlated with training-induced rs-FC changes between the MT+ and right PoG ($r = -0.49$, $P = 0.028$, uncorrected). Additionally, to examine whether the combined two opposing changes of cortical and subcortical regions could predict the behavioral learning effects, we extracted principal components (PC) from positive and negative connectivity change maps. Next, the simple regression analysis was conducted to predict accuracy based on the combined first PCs of each opposing changes. This was repeated with other behavioral indices such as reaction time and IE as well. The results did not show significant regression equation for the dependent variables (ACC: $P = 0.83$, $R^2 = 0.02$; RT: $P = 0.71$, $R^2 = 0.04$; IE: $P = 0.78$, $R^2 = 0.03$).
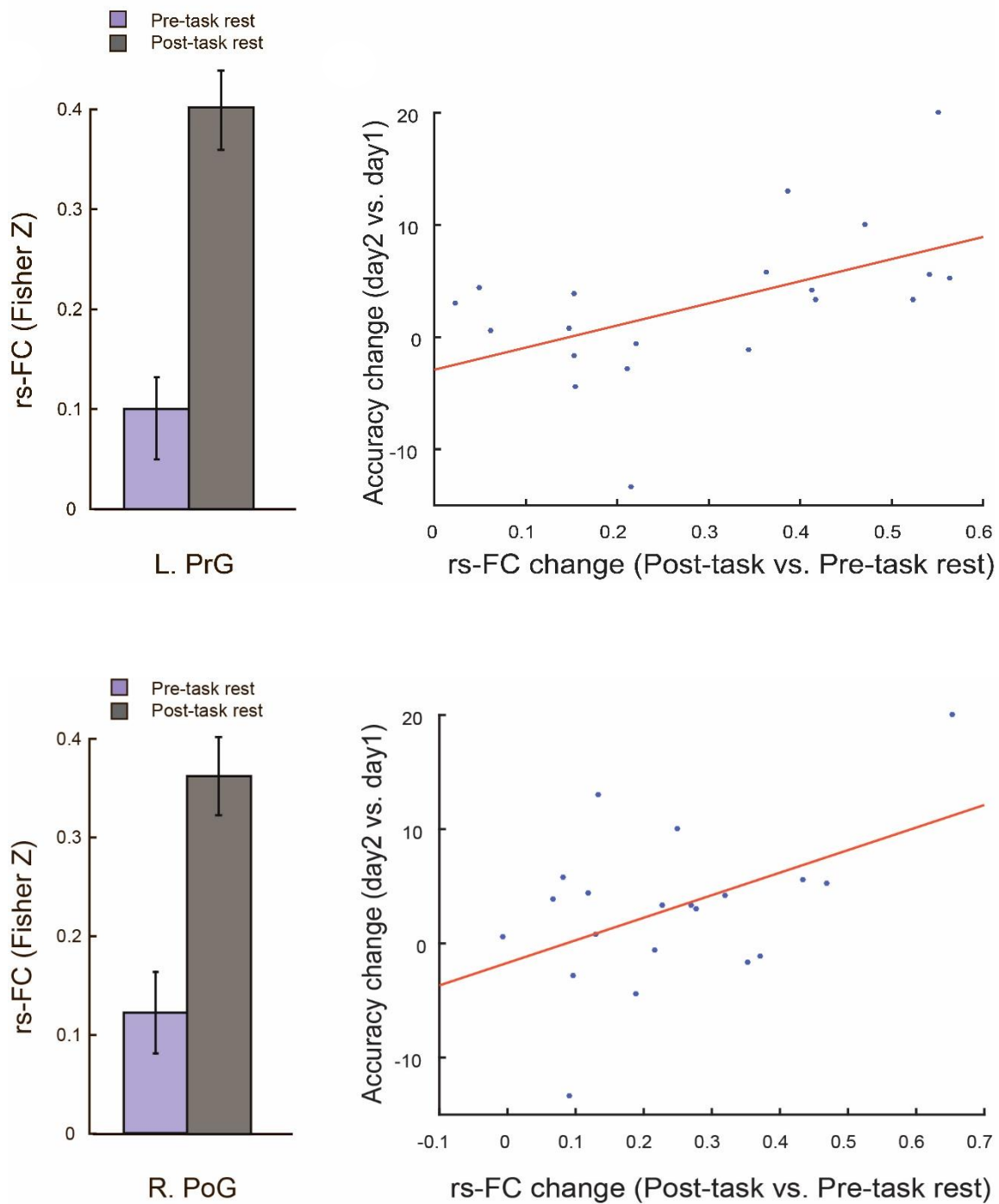
Figure 12. Brain-behavior correlation.
Pre-task and post-task rs-FC between the MT+ and left PrG and right PoG. The y-axis indicates the correlations (Fisher Z transformed) between the time series extracted from the MT+ and left PrG and right PoG, averaged across participants. The error bars indicate s.e.m. The bar graph is provided for visualization purposes, and no statistical test was applied to this data. Scatter plots showing individual differences in behavioural improvement (accuracy gain on day 2 relative to day 1) as a function of training-induced rs-FC change.

Table 5. Brain-behavior correlation (MT+, Accuracy)
Brain-behavior correlation in regions showing training-induced rs-FC changes with MT+ seed: Accuracy gain was used as the behavioral index.

Region	Hemi	*r* value	*P*-value
Post-task rest > Pre-task rest			
Postcentral gyrus	R	0.023	0.924
Postcentral gyrus	R	0.089	0.710
Postcentral gyrus	L	0.047	0.844
Inferior temporal gyrus	L	−0.111	0.643
Middle temporal gyrus	L	0.087	0.715
Superior temporalgyrus	L	0.091	0.703
Planum temporale	L	0.133	0.576
Superior frontal gyrus	L	−0.188	0.427
Postcentral gyrus	R	0.471	0.036
Middle temporal gyrus	R	0.063	0.790
Precentral gyrus	L	0.522	0.018
Central opercular cortex	R	0.110	0.645
Pre-task rest > Post-task rest			
Thalamus[*]	L	0.005	0.984
Thalamus[*]	L	0.145	0.542
Thalamus[*]	R	0.019	0.935
Thalamus[*]	R	0.127	0.592
Thalamus[*]	L	−0.206	0.384
Thalamus[*]	R	0.263	0.263
Putamen[*]	R	0.230	0.330

Anatomical labels derived from Harvard-Oxford cortical structural atlas. [*]Labels derived from Harvard-Oxford Subcortical structural atlas. L = left hemisphere, R = right hemisphere.

Table 6. Brain-behavior correlation (MT+, RT)
Brain-behavior correlation in regions showing training-induced rs-FC changes with MT+ seed: Reaction time was used as the behavioral index.

Region	Hemi	r value	P-value
Post- vs. Pre-task rest			
Postcentral gyrus	R	0.243	0.301
Postcentral gyrus	R	0.001	0.997
Postcentral gyrus	L	0.269	0.252
Inferior temporal gyrus	L	−0.074	0.757
Middle temporal gyrus	L	−0.119	0.616
Superior temporal gyrus	L	0.080	0.736
Planum temporale	L	−0.232	0.324
Superior frontal gyrus	L	0.328	0.158
Postcentral gyrus	R	−0.168	0.479
Middle temporal gyrus	R	−0.090	0.706
Precentral gyrus	L	−0.180	0.448
Central opercular cortex	R	−0.298	0.202
Post- vs. Pre-task rest			
Thalamus[*]	L	−0.114	0.633
Thalamus[*]	L	−0.310	0.184
Thalamus[*]	R	−0.230	0.329
Thalamus[*]	R	−0.217	0.359
Thalamus[*]	L	−0.061	0.797
Thalamus[*]	R	−0.271	0.247
Right Putamen[*]	R	0.035	0.885

Anatomical labels derived from Harvard-Oxford cortical structural atlas (* = Harvard-Oxford subcortical structural atlas). L= left hemisphere, R = right hemisphere.

Table 7. Brain-behavior correlation (MT+, IE)
Brain-behavior correlation in regions showing training-induced rs-FC changes with MT+ seed: Inverse Efficiency was used as the behavioral index.

Region	Hemi	*r* value	*P*-value
Post- vs. Pre-task rest			
Postcentral gyrus	R	0.017	0.943
Postcentral gyrus	R	−0.116	0.626
Postcentral gyrus	L	0.066	0.783
Inferior temporal gyrus	L	0.095	0.690
Middle temporal gyrus	L	−0.110	0.645
Superior temporal gyrus	L	− 0.046	0.848
Planum temporale	L	−0.198	0.403
Superior frontal gyrus	L	0.218	0.356
Postcentral gyrus	R	−0.490	0.028
Middle temporal gyrus	R	−0.065	0.785
Precentral gyrus	L	−0.480	0.032
Central opercular cortex	R	−0.223	0.344
Post- vs. Pre-task rest			
Thalamus[*]	L	−0.072	0.763
Thalamus[*]	L	−0.260	0.269
Thalamus[*]	R	−0.120	0.615
Thalamus[*]	R	− 0.212	0.369
Thalamus[*]	L	0.071	0.765
Thalamus[*]	R	−0.317	0.174
Right Putamen[*]	R	−0.220	0.352

4.5 Rs-FC and activation change correlation

Finally, we tested whether the training-induced rs-FC change in the MT+ predicts individuals' task activation change (i.e., accuracy gain) on day 2. The correlation between task activation change (from day 1 to day 2) and rs-FC change conducted. However, given that we observed some significant correlations between rs-FC changes and activation changes in thalamus, postcentral gyrus, the results did not survive after multiple comparison corrections (see Tables 8-11).

Table 8. Task-Rest fMRI correlation (MT+ seed, MT+ activation change)
Task-Rest fMRI correlation in regions showing training-induced rs-FC changes with MT+ seed and MT+ activation change.

Region	Hemi	r value	P-value
Post- vs. Pre-task rest			
Postcentral gyrus	R	−0.278	0.235
Postcentral gyrus	R	0.346	0.134
Postcentral gyrus	L	−0.323	0.164
Inferior temporal gyrus	L	−0.025	0.918
Middle temporal gyrus	L	−0.042	0.859
Superior temporal gyrus	L	−0.420	0.065
Planum temporale	L	−0.139	0.559
Superior frontal gyrus	L	−0.031	0.896
Postcentral gyrus	R	0.171	0.471
Middle temporal gyrus	R	−0.107	0.653
Precentral gyrus	L	0.029	0.903
Central opercular cortex	R	0.148	0.533
Post- vs. Pre-task rest			
Thalamus[*]	L	0.357	0.122
Thalamus[*]	L	0.472	0.035
Thalamus[*]	R	0.272	0.246
Thalamus[*]	R	0.260	0.268
Thalamus[*]	L	0.562	0.010
Thalamus[*]	R	0.310	0.184
Right Putamen[*]	R	0.298	0.202

Table 9. Task-Rest fMRI correlation (MT+ seed, dACC activation change)

Task-Rest fMRI correlation in regions showing training-induced rs-FC changes with MT+ seed and dACC activation change.

Region	Hemi	*r* value	*P*-value
Post- vs. Pre-task rest			
Postcentral gyrus	R	−0.504	0.023
Postcentral gyrus	R	−0.296	0.205
Postcentral gyrus	L	−0.068	0.777
Inferior temporal gyrus	L	−0.105	0.659
Middle temporal gyrus	L	−0.186	0.433
Superior temporal gyrus	L	−0.261	0.267
Planum temporale	L	−0.026	0.913
Superior frontal gyrus	L	−0.229	0.332
Postcentral gyrus	R	−0.196	0.407
Middle temporal gyrus	R	0.007	0.978
Precentral gyrus	L	−0.084	0.724
Central opercular cortex	R	0.009	0.971
Post- vs. Pre-task rest			
Thalamus[*]	L	0.147	0.537
Thalamus[*]	L	0.049	0.837
Thalamus[*]	R	0.118	0.621
Thalamus[*]	R	0.062	0.796
Thalamus[*]	L	0.046	0.846
Thalamus[*]	R	0.081	0.735
Right Putamen[*]	R	−0.156	0.512

Table 10. Task-Rest fMRI correlation (MT+ seed, Right Ins activation change)
Task-Rest fMRI correlation in regions showing training-induced rs-FC changes with MT+ seed and right insula activation change.

Region	Hemi	r value	P-value
Post- vs. Pre-task rest			
Postcentral gyrus	R	−0.457	0.043
Postcentral gyrus	R	0.044	0.853
Postcentral gyrus	L	−0.418	0.067
Inferior temporal gyrus	L	−0.202	0.393
Middle temporal gyrus	L	−0.081	0.736
Superior temporal gyrus	L	−0.337	0.146
Planum temporale	L	−0.287	0.220
Superior frontal gyrus	L	−0.319	0.170
Postcentral gyrus	R	−0.029	0.903
Middle temporal gyrus	R	−0.231	0.328
Precentral gyrus	L	−0.186	0.432
Central opercular cortex	R	−0.065	0.785
Post- vs. Pre-task rest			
Thalamus[*]	L	0.473	0.035
Thalamus[*]	L	0.316	0.174
Thalamus[*]	R	0.293	0.211
Thalamus[*]	R	0.328	0.159
Thalamus[*]	L	0.397	0.083
Thalamus[*]	R	0.384	0.094
Right Putamen[*]	R	0.326	0.161

Table 11 Task-Rest fMRI correlation (MT+ seed, Left Ins activation change)
Task-Rest fMRI correlation in regions showing training-induced rs-FC changes with MT+ seed and left insula activation change.

Region	Hemi	r value	P-value
Post- vs. Pre-task rest			
Postcentral gyrus	R	−0.531	0.016
Postcentral gyrus	R	−0.034	0.887
Postcentral gyrus	L	−0.249	0.289
Inferior temporal gyrus	L	−0.200	0.397
Middle temporal gyrus	L	−0.399	0.082
Superior temporal gyrus	L	−0.312	0.180
Planum temporale	L	−0.426	0.061
Superior frontal gyrus	L	−0.153	0.521
Postcentral gyrus	R	0.028	0.908
Middle temporal gyrus	R	−0.170	0.474
Precentral gyrus	L	−0.165	0.487
Central opercular cortex	R	−0.382	0.096
Post- vs. Pre-task rest			
Thalamus[*]	L	0.368	0.110
Thalamus[*]	L	0.096	0.686
Thalamus[*]	R	0.346	0.134
Thalamus[*]	R	0.237	0.315
Thalamus[*]	L	0.223	0.344
Thalamus[*]	R	0.249	0.289
Right Putamen[*]	R	0.039	0.870

Chapter 5

DISCUSSION AND FUTURE WORK

5.1   Feature-specific resting-state functional connectivity change

While most previous fMRI studies on VPL have investigated task-related brain activation [2,9], offline processes following task periods are also known to be important for VPL [10,11,22]. For instance, a previous study revealed an fMRI signal increase in the early visual cortex (V1) during sleep after visual perceptual training [12]. This elevated fMRI signal in the feature representation region may indicate a spontaneous reactivation of the trained visual feature and the consolidation process during sleep. Recent studies further show that training-induced fMRI signal changes are observed even during wakeful resting periods immediately after the task session [13,14,46]. In particular, Urner *et al.* (2013) [25] showed that brief training on a visual motion discrimination task (~90 min) induced a significant increase in rs-FC between the hippocampus and striatum immediately after training. However, they did not observe training-induced rs-FC changes in visual feature representation regions, leaving it unclear whether visual feature representation regions show offline rs-FC changes during the early learning period.

The current study provides the first direct evidence of rapid training-induced rs-FC changes in the MT+ immediately after training on a visual motion discrimination task. One possible explanation for the lack of rs-FC changes in the MT+ in the previous study is that only low-coherence (20%) visual motion stimuli and control static dots were used. In the current study, we used high- as well as low-coherence visual motion stimuli, which might have facilitated offline reactivation in the MT+.

5.2   Model specification

The current finding that training-induced rs-FC changes were specifically observed in the MT+ is of particular interest. One of the long-standing questions regarding the mechanisms underlying VPL is the distinct roles of visual feature-representation regions and higher-order cognitive regions. Some studies have emphasized the critical roles of learning-induced plasticity in visual feature-specific areas ("visual model"), whereas other studies have reported that higher-order cognitive regions involved in decision making (including the dACC) also play key roles ("cognitive model") [7]. Although both types of the region are likely to contribute to VPL [47], recent evidence suggests that specific fMRI signal patterns induced in the early visual cortex during offline periods (i.e., without explicit perceptual discrimination tasks) are sufficient for VPL [48]. Our current findings are consistent with this notion, revealing that the visual feature representation regions are specifically plastic and exhibit rapid rs-FC changes immediately after a brief period of visual perceptual training.

5.3 History replaying role of resting-state functional connectivity

The role of experience-induced rs-FC changes immediately after tasks is a topic of current interest across a range of research domains, including episodic memory encoding and motor learning [13,15,49]. Many recent studies have reported that rs-FC during passive, wakeful rest periods reflect preceding visual/cognitive experience [50-53]. These experience-induced resting-state fMRI signals appear to reflect spontaneous reactivation of recent experiences and offline consolidation processes, thereby contributing to the subsequent behavioural performance of memory and learning. For example, a previous study revealed that rs-FC immediately after memory encoding tasks increased in the medial temporal lobe (including the hippocampus), which further predicted memory performance the next day [21]. Another study reported that a short period of sensorimotor learning-induced a rapid increase in rs-FC among the frontoparietal regions and cerebellum [19]. Taken together with the current finding of MT+ specific rs-FC reconfiguration after visual perceptual training, these results suggest that experience-induced plastic changes in rs-FC during a wakeful rest period immediately after task performance may reflect offline processes that are critically important for many different types of memory and learning.

If training-induced rs-FC changes immediately after tasks play a key role in early consolidation processes, the rs-FC changes during this period may predict subsequent performance improvements (e.g., ~24 hours after training). Inspired by similar findings in recent memory research [21] we tested this possibility by examining the relationship between training-induced rs-FC changes and performance improvements on day 2 (relative to day 1). We obtained a suggestive result that the rs-FC change between the MT+ and motor-related region (i.e., the precentral gyrus) was correlated with behavioural improvement, although this result did not survive multiple comparison correction and should be interpreted with caution.

5.4   Different temporal profiles of learning and different results

A notable characteristic of the current results is the significant increase in rs-FC between the MT+ and the widespread cortical regions (e.g., sensorimotor and temporal cortices) after training. This is in contrast to the findings of a previous study, which showed a decrease in rs-FC between the visual feature representation regions and dorsal attention system [24]. This apparent discrepancy may be related to the different temporal structure of visual perceptual training and the intervals between training and resting-state fMRI scans. Specifically, the previous study involved several days of intensive visual perceptual training (2–9 days) and examined rs-FC changes well after the learning was established. In contrast, the current study focused on the effects of a single session of short-term visual perceptual training (~30 min), and examined rs-FC changes in the early learning phase, immediately after the task session. Previous studies investigating post-task rs-FC change immediately after training have generally reported increased rs-FC in regions specifically related to the task performed [19,25]. Interestingly, previous studies investigating training-dependent changes in task-related fMRI activation have also reported similar distinct profiles depending on early vs. late learning phases [56]. For example, one study showed that V1 activation during the visual perceptual task markedly increased during a relatively early phase of learning, then decreased and returned to baseline during a later learning phase [56].

The current findings may indicate that training-induced rs-FC changes exhibit a similar temporal profile depending on early/late learning phases. This issue is an interesting research target for future studies. It is also notable that we found a training-induced decrease in rs-FC between the MT+ and subcortical regions (e.g., the thalamus), which was the opposite of what we observed in the sensorimotor and temporal cortices. According to a previous study, stimulus-induced activation after VPL and one-night sleep was positively correlated with post-training behavioral performance in the precentral and middle temporal gyri whereas negatively correlated in the thalamus [11]. In line with this previous report, our results suggest opposing contributions of cortical and subcortical regions to offline consolidation processes of VPL.

5.5   Dissociation between learning and adaptation

It has been shown that VPL can be distinguished from visual adaptation, another form of short-term perceptual plasticity, although recent evidence suggests that the boundary between the two types of plasticity is more ambiguous than previously thought [57]. To discriminate VPL from adaptation, one typical experimental procedure is to examine the specificity of brain response changes to trained vs. untrained visual features [9,24,56]. However, it is difficult to perform such analyses in the current experimental design. Nonetheless, this issue may be partially addressed by considering that there was no significant activation decrease in area MT+ or behavioral improvement (two characteristic components of adaptation) in the course of the 6 runs of t-fMRI on day 1 (see Table 2). These observations suggest that the current results would not involve adaptation effects.

5.6   Other future avenues

(a)   Here, we did not have prior knowledge about which brain regions would show performance-dependent rs-FC changes with the MT+. From a post-hoc perspective, our findings seem to suggest that spontaneous coactivation between the MT+ and motor cortex during the post-task rest reflect (or facilitate) the offline consolidation process that associate specific visual features with motor outputs. Our findings may serve as a foundation for future studies to formally test the relationship between training-induced rs-FC changes in specific brain regions during the early learning phase (i.e., immediately after training) and performance improvement in later phases (over days). Moreover, graph analysis [54,55] could be useful for examining the relationship between rapid reorganization of large-scale functional brain networks immediately after training and subsequent behavioural improvement.

(b)   Here, we focused on VPL of basic primitive features, such as motion direction. However, to what extent is learning of primitive feature generalizable for more complex features like semantic processing, categorization learning, and other types of learning? This challenging question leads a clear future pathway from our findings in the way that if the complex features with their own distinguishing characteristics have basically common aspects

of mechanisms shared by learning of primitive features, the generalization aspect of neuroplasticity would largely be addressed accordingly. The degree of transferring depends on neural pathways: The transfer of learning from one task to another depends on some degree of overlap in neural processing pathways as well as on the complexity of the visual training tasks involved.

(d)   Vision is a whole body experience, what we touch influences how we see. Taste is affected by our sense of smell. Our sight informs how we hear. Our senses depend on each other. So our findings in resting state functional connectivity change, clearly show primary sensory regions such as premotor and auditory cortices have a stronger connection with MT+ (visual cortex) after task. This notion can also be considered as a future study to further investigating cross-modal perception.

(e)   Why do some of us learn things more easily than others? by addressing this central question, it would allow developing new and more effective interventions regarding individual patterns and variability in learning and neuroplasticity as it can be seen from fig 7. A fuller understanding of VPL also has implications for clinical applications and is vital for patients with weak or degraded vision.

Chapter 6

CONCLUSION

In conclusion, our study revealed that a brief period of visual perceptual training induces rapid rs-FC changes immediately after training in visual feature representation regions, but not in higher-order cognitive regions. This finding provides further support for the distinct roles of visual feature representation regions and decision-related regions in VPL, with a particular emphasis on offline plasticity in feature representation regions during the early learning phase. In a broader context, our study highlights the critical role of experience-induced plasticity during wakeful rest periods immediately after tasks, which may contribute to various types of memory and learning, ranging from VPL to motor skill acquisition and episodic memory formation [10,22,57].

When you complete reading this thesis, your brain will not be the same as when you started [59]

I think that's pretty amazing

REFERENCES

1. Karni A, Sagi D. Where practice makes perfect in texture discrimination: evidence for primary visual cortex plasticity. Proc Natl Acad Sci U S A. 1991;88(11):4966–70.

2. Schwartz S, Maquet P, Frith C. Neural correlates of perceptual learning : A functional MRI study of visual texture discrimination. Proc Natl Acad Sci. 2002;99(26):17137–42.

3. Watanabe T, Yuka Sasaki. Perceptual learning: Toward a comprehensive theory. Annu Rev Psychol. 2015;66:197–221.

4. Sasaki Y, Nanez JE, Watanabe T. Advances in visual perceptual learning and plasticity. Nat Rev Neurosci. 2010;11(1):53.

5. Shibata K, Sasaki Y, Kawato M, Watanabe T. Neuroimaging Evidence for 2 Types of Plasticity in Association with Visual Perceptual Learning. Cereb Cortex. 2016;26:3681–9.

6. Shibata K, Sasaki Y, Bang JW, Walsh EG, Machizawa MG, Tamaki M, et al. Overlearning hyperstabilizes a skill by rapidly making neurochemical processing inhibitory-dominant. Nat Neurosci. 2017;20(3):470.

7. Shibata K, Sagi D, Watanabe T. Two-stage model in perceptual learning: Toward a unified theory. Ann N Y Acad Sci. 2014;1316(1):18–28.

8. Chen N, Bi T, Zhou T, Li S, Liu Z, Fang F. Sharpened cortical tuning and enhanced cortico-cortical communication contribute to the long-term neural mechanisms of visual

motion perceptual learning. Neuroimage. 2015;115:17–29.

9. Sigman M, Pan H, Yang Y, Stern E, Silbersweig D, Gilbert CD. Top-down reorganization of activity in the visual pathway after learning a shape identification task. Neuron. 2005;46(5):823–35.

10. Stickgold R. Sleep-dependent memory consolidation. Nature. 2005;437(7063):1272–8.

11. Walker MP, Stickgold R, Jolesz FA, Yoo SS. The functional anatomy of sleep-dependent visual skill learning. Cereb Cortex. 2005;15(11):1666–75.

12. Yotsumoto Y, Sasaki Y, Chan P, Vasios CE, Bonmassar G, Ito N, et al. Location-Specific Cortical Activation Changes during Sleep after Training for Perceptual Learning. Curr Biol. 2009;19(15):1278–82.

13. Tambini A, Ketz N, Davachi L. Enhanced Brain Correlations during Rest Are Related to Memory for Recent Experiences. Neuron. 2010;65(2):280–90.

14. Stevens WD, Buckner RL, Schacter DL. Correlated low-frequency BOLD fluctuations in the resting human brain are modulated by recent experience in category-preferential visual regions. Cereb Cortex. 2010;20(8):1997–2006.

15. Vahdat S, Darainy M, Milner TE, Ostry DJ. Functionally Specific Changes in Resting-State Sensorimotor Networks after Motor Learning. J Neurosci. 2011;31(47):16907–15.

16. Power JD, Schlaggar BL, Fair D a, Petersen SE. The development of human functional brain networks. Neuron. 2010;67(5):735–48.

17. Greicius MD, Krasnow B, Reiss AL, Menon V. Functional connectivity in the resting brain: a network analysis of the default mode hypothesis. Proc Natl Acad Sci. 2003;100(1):253–8.

18. Biswal B, Yetkin FZ, Haughton VM, Hyde JS. Functional connectivity in the motor cortex of resting human brain using echo-planar MRI. Magn Reson Med. 1995;34(4):537–41.

19. Albert NB, Robertson EM, Miall RC. The Resting Human Brain and Motor Learning. Curr Biol. 2009;19(12):1023–7.

20. Gregory MD, Agam Y, Selvadurai C, Nagy A, Tucker M, Robertson EM, et al. Resting state connectivity immediately following learning correlates with subsequent sleep-dependent enhancement of motor task performance. NeuroImage. 2014;102(2):666–73.

21. Murty VP, Tompary A, Adcock RA, Davachi L. Selectivity in Postencoding Connectivity with High-Level Visual Cortex Is Associated with Reward-Motivated Memory. J Neurosci. 2017;37(3):537–45.

22. Walker MP, Stickgold R. Sleep, Memory, and Plasticity. Annu Rev Psychol. 2006;57:139–66.

23. Guerra-Carrillo B, Allyson P. Mackey, Silvia A. Bunge. Resting-State fMRI : A Window into Human Brain Plasticity Resting-State fMRI : A Window into Human Brain Plasticity. Neurosci. 2014;20(5)522–33.

24. Lewis CM, Baldassarre A, Committeri G, Luca G. Learning sculpts the spontaneous activity of the resting human brain. Proc Natl Acad Sci. 2009;106(41):17558–63.

25. Urner M, Samuel D, Friston K, Rees G. Early visual learning induces long-lasting connectivity changes during rest in the human brain. Neuroimage. 2013;77:148–56.

26. Shadlen MN, Newsome WT. Motion perception: seeing and deciding. Proc Natl Acad Sci U S A. 1996;93(2):628–33.

27. Shadlen MN, Britten KH, Newsome WT, Movshon J a. A computational analysis of the relationship between neuronal and behavioral responses to visual motion. J Neurosci. 1996;16(4):1486–510.

28. Newsome WT, Park EB. A Selective Impairment of Motion Perception Following Lesions of the Middle Temporal Visual Area (MT). J Neurosci. 1988;8(6):2201–11.

29. Amano K, Wandell BA, Dumoulin SO. Visual Field Maps, Population Receptive Field Sizes, and Visual Field Coverage in the Human MT+ Complex. J Neurophysiol. 2009;102(5):2704–18.

30. Heeger DJ, Boynton GM, Demb JB, Seidemann E, Newsome WT. Motion opponency in visual cortex. J Neurosci. 1999;19(16):7162–74.

31. Beauchamp MS, Cox RW, DeYoe EA. Graded effects of spatial and featural attention on human area MT and associated motion processing areas. J Neurophysiol. 1997;78(1):516–20.

32. Tootell RB, Reppas JB, Dale AM, Look RB, Sereno MI, Malach R, et al. Visual motion aftereffect in human cortical area MT revealed by functional magnetic resonance imaging. Nature. 1995; 375(6527):139–41.

33. Britten KH, William T. Newsome, Michael N. Shadlen, Simona Celebrini, J. Anthony Movshon. A relationship between behavioral choice and the visual responses of neurons in macaque MT. Vis Neurosci. 1996;13(1):87–100.

34. Brainard DH. The Psychophysics Toolbox. Spat Vis. 1997;10(4):433–6.

35. Pelli DG. The VideoToolbox software for visual psychophysics: transforming numbers into movies. Spat Vis. 1997; 10(4):437–42.

36. Chen MY, Jimura K, White CN, Maddox WT, Poldrack RA. Multiple brain networks

contribute to the acquisition of bias in perceptual decision-making. Front Neurosci. 2015;9:63.

37. Britten KH, Shadlen MN, Newsome WT, Movshon J a. The analysis of visual motion: a comparison of neuronal and psychophysical performance. J Neurosci. 1992;12(12):4745–65.

38. Palmer J, Huk AC, Shadlen MN. The effect of stimulus strength on the speed and accuracy of a perceptual decision. J Vis. 2005;5(5):376–404.

39. Worsley KJ, Friston KJ. Analysis of fMRI Time-Series Revisited—Again. Neuroimage. 1995;2(3):173–81.

40. Harmelech T, Preminger S, Wertman E, Malach R. The Day-After Effect: Long Term, Hebbian-Like Restructuring of Resting-State fMRI Patterns Induced by a Single Epoch of Cortical Activation. J Neurosci. 2013;33(22):9488–97.

41. Lakens D. Calculating and reporting effect sizes to facilitate cumulative science: A practical primer for t-tests and ANOVAs. Front Psychol. 2013;4:1–12.

42. Erickson DT, Kayser AS. The neural representation of sensorimotor transformations in a human perceptual decision making network. Neuroimage. 2013;79:340–50.

43. Kayser AS, Buchsbaum BR, Erickson DT, Esposito MD. The Functional Anatomy of a Perceptual Decision in the Human Brain. J Neurophysiol. 2010;103(3):1179–94.

44. Keuken MC, Müller-Axt C, Langner R, Eickhoff SB, Forstmann BU, Neumann J. Corrigendum: Brain networks of perceptual decision-making: an fMRI ALE meta-analysis. Front Hum Neurosci. 2017;11:1–14.

45. Lamichhane B, Adhikari BM, Dhamala M. The activity in the anterior insulae is modulated by perceptual decision-making difficulty. Neuroscience. 2016;327:79–94.

46. Vilsten JS, Mundy ME. Imaging early consolidation of perceptual learning with face stimuli during rest. Brain Cogn. 2014;85(1):170–9.

47. Kahnt T, Grueschow M, Speck O, Haynes J-D. Perceptual Learning and Decision-Making in Human Medial Frontal Cortex. Neuron. 2011;70(3):549–59.

48. Shibata K, Watanabe T, Sasaki Y, Kawato M. Perceptual Learning Incepted by Decoded fMRI Neurofeedback Without Stimulus Presentation. Science. 2011;334(6061):1413–5.

49. Sami S, Robertson EM, Miall RC. The Time Course of Task-Specific Memory Consolidation Effects in Resting State Networks. J Neurosci. 2014;34(11):3982–92.

50. Mennes M, Kelly C, Zuo XN, Di Martino A, Biswal BB, Castellanos FX, et al. Inter-individual differences in resting-state functional connectivity predict task-induced BOLD activity. Neuroimage. 2010;50(4):1690–701.

51. Eryilmaz H, Van De Ville D, Schwartz S, Vuilleumier P. Impact of transient emotions on functional connectivity during subsequent resting state: A wavelet correlation approach. Neuroimage. 2011;54(3):2481–91.

52. Waites AB, Stanislavsky A, Abbott DF, Jackson GD. Effect of prior cognitive state on resting state networks measured with functional connectivity. Hum Brain Mapp. 2005;24(1):59–68.

53. Kelly C, Castellanos FX. Strengthening connections: Functional connectivity and brain plasticity. Neuropsychol Rev. 2014;24(1):63–76.

54. Kahn AE, Mattar MG, Vettel JM, Wymbs NF, Grafton ST, Bassett DS. Structural Pathways Supporting Swift Acquisition of New Visuomotor Skills. Cereb Cortex. 2017;27(1):173–84.

55. Bassett DS, Yang M, Wymbs NF, Grafton ST. Learning-Induced Autonomy of

Sensorimotor Systems. Nat Neurosci. 2015;18(5):744–51.

56. Yotsumoto Y, Watanabe T, Sasaki Y. Different Dynamics of Performance and Brain Activation in the Time Course of Perceptual Learning. Neuron. 2008;57(6):827–33.

57. Webster MA. Adaptation and visual coding. J Vis. 2011;11:1-23.

58. Censor N, Sagi D, Cohen LG. Common mechanisms of human perceptual and motor learning. Nat Rev Neurosci. 2012;13(9):658–64.

59. Boyd L. After watching this, your brain will not be the same. TEDxVancouver. 2015. Link: https://www.youtube.com/watch?v=LNHBMFCzznE

60. Genetic Science Learning Center. Neurons Transmit Messages In The Brain. Link: http://learn.genetics.utah.edu/content/neuroscience/neurons/

61. Moore DR, Amitay S, Hawkey DJ. Auditory perceptual learning. Learn Mem. 2003; 10: 83-85.

62. Dinse HR, Ragert P, Pleger B, Schwenkreis P, Tegenthoff M. Pharmacological modulation of perceptual learning and associated cortical reorganization. Science. 2003; 301: 91-94.

63. McLaren, G. (2014). Foundations of Behavioral Neuroscience [PowerPoint slides]. http://www2.bakersfieldcollege.edu/gleblanc/Biological%20Psychology/Bio%20Psyc%20lectures/Carlson%20ppts/C12_Carlson9e.ppt

64. Adini Y, Sagi D, Tsodyks M. Context-enabled learning in the human visual system. Nature. 2002; 415: 790-793.

65. Tsodyks M, Adini Y, Sagi D. Associative learning in early vision. Neural Netw. 2004; 17: 823-832.

66. Yotsumoto Y, Watanabe T. Defining a link between perceptual learning and attention. PLoS Biol. 2008; 6(8): e221. doi:10.1371.

67. Dosher BA, Lu ZL. Mechanisms of perceptual learning. Vision Res. 1999; 39: 3197-3221.

68. Ahissar M, Hochstein S. The reverse hierarchy theory of visual perceptual learning. Trends Cogn Sci. 2004; 8: 457-464.